

ULRR

The biocompatibility of mesoporous silicates

Item Type	Article
Authors	Hudson, Sarah;Padera, Robert F;Langer, Robert;Kohane, Daniel S.
Citation	Biomaterials;29 (30), pp. 4045-4055
Publisher	Elsevier
Download date	2026-05-12 00:37:20
Item License	https://creativecommons.org/licenses/by-nc-sa/1.0/
Link to Item	https://hdl.handle.net/10344/5016

Published in final edited form as:

Biomaterials. 2008 October ; 29(30): 4045–4055. doi:10.1016/j.biomaterials.2008.07.007.

THE BIOCOMPATIBILITY OF MESOPOROUS SILICATES

Sarah Hudson^{1,2}, Robert F. Padera³, Robert Langer¹, and Daniel S. Kohane^{4*}

¹*Department of Chemical Engineering, Massachusetts Institute of Technology, 77 Massachusetts Ave., Cambridge, MA 02139.* ²*Materials and Surface Science Institute, University of Limerick, Castletroy, Limerick, Ireland.* ³*Department of Pathology, Brigham and Women's Hospital, Boston, MA 02115*

⁴*Laboratory for Biomaterials and Drug Delivery, Department of Anesthesiology, Division of Critical Care Medicine, Children's Hospital, Harvard Medical School, 300 Longwood Ave., Boston, MA 02115*

Abstract

Micro- and nano- mesoporous silicate particles are considered potential drug delivery systems because of their ordered pore structures, large surface areas and the ease with which they can be chemically modified. However, few cytotoxicity or biocompatibility studies have been reported, especially when silicates are administered in the quantities necessary to deliver low-potency drugs. The biocompatibility of mesoporous silicates of particle sizes ~ 150 nm, ~ 800 nm and ~ 4 μm and pore sizes of 3 nm, 7 nm and 16 nm respectively are examined here. In vitro, mesoporous silicates showed a significant degree of toxicity at high concentrations with mesothelial cells. Following subcutaneous injection of silicates in rats, the amount of residual material decreased progressively over three months, with good biocompatibility on histology at all time points. In contrast, intra peritoneal and intra venous injections in mice resulted in death or euthanasia. No toxicity was seen with subcutaneous injection of the same particles in mice. Microscopic analysis of the lung tissue of the mice indicates that death may be due to thrombosis. Although local tissue reaction to mesoporous silicates was benign, they caused severe systemic toxicity. This toxicity could be mitigated by modification of the materials.

Introduction

Mesoporous silicates have been studied in the context of drug delivery [1–29], drug targeting [30,31], tissue engineering [32–35], gene transfection [36–38] and cell tracking [39–42]. The unique mesoporous structure of these particles is the cause of the broad interest in their application in biotechnology. Their large internal volumes, high surface areas and straight narrow channels allow for the high adsorption of drugs and proteins into their structures. The straight channels allow for adsorbed drugs to diffuse out in a controlled manner over time frames that depend on the drug in question (size and chemical composition), the release medium, pore size, surface functionalization and particle size and morphology. Drug release can occur over minutes, hours or days [2,5–7]. Mesoporous materials also offer the advantage that the channels can be used as a reservoir and the openings can be opened or closed by different systems, e.g. polymers [3,9,19,20,30,43,44], nanocrystals [1] or photoactive derivatives [45]. Triggers such as heat [19,43], pH [3,20,30,44], light [45], chemicals [1],

*Corresponding author. Phone: 617-355-7327, FAX: 617-730-0453, Email: daniel.kohane@childrens.harvard.edu.

Publisher's Disclaimer: This is a PDF file of an unedited manuscript that has been accepted for publication. As a service to our customers we are providing this early version of the manuscript. The manuscript will undergo copyediting, typesetting, and review of the resulting proof before it is published in its final citable form. Please note that during the production process errors may be discovered which could affect the content, and all legal disclaimers that apply to the journal pertain.

ultrasound[9] or magnetism[46] can be used to control drug release. Consequently, there have been numerous studies of release profiles of drugs from micro- and nano- mesoporous silicates into simulated body fluid or phosphate buffered saline [1–30].

The biological response to these materials has been much less well characterized. Several reviews suggest that silica nanoparticles (solgels, xerogels, etc) are biocompatible and degrade over time in the body [12,25,47,48]. The walls of mesoporous silicates have the same amorphous silica composition but less is known regarding their inherent biocompatibility and biodegradability. *In vitro* cytotoxicity studies exhibit low toxicity at low concentrations [1, 15,17,36,37,39,40] but this toxicity appears to increase at higher concentrations [37]. The toxicity has been shown to depend somewhat on particle size [24]. *In vivo* studies with mesoporous particles 1–2 μm in size have shown little toxicity in small quantities, 1.1 mg and $\sim 4 \times 10^7$ particles (SBA-type (SBA: Santa Barbara Amorphous) and MCM-type (MCM: Mobil Composition of Matter) respectively) [2,37]. Mesoporous particles (~ 100 nm) fused with iron oxide amorphous silica particles exhibited low toxicity intravenously in mice [41].

The principal purpose of this research is to evaluate the toxicity of mesoporous silicates specifically as drug delivery vehicles. In that context, it is important to note that many drug delivery systems, particularly for local depot applications or for drugs with low potency, may require considerable amounts of particle to be delivered. For example, poly (lactic-co-glycolic) acid (PLGA) microparticles loaded with bupivacaine – a relatively potent local anesthetic – are injected at the sciatic nerve in quantities greater than 200 mg/kg, even though they have a 75% loading with the drug[49]. Similarly, effective coverage of a large body cavity such as the peritoneum or pleura could require large quantities of particle[50]. In the context of the peritoneum, we have shown that even massive quantities of PLGA micro and nanoparticles (100 mg in a 25 g mouse, or 4 g/kg) are well tolerated, although adhesions form in some cases [50]. Lesser but still substantial quantities (10 mg) of other types of particles are also tolerated in the peritoneum[51].

Here, we examine the cytotoxicity and biocompatibility of mesoporous silicates that have been used in biotechnological applications [1–21,23–30,32,33,35–40,43,44,46,47], such as the MCM-41 and SBA-15. We also examine MCF (MCF: Mesocellular Foam) which is an SBA-type material with a larger, more disordered pore system[9,52]. The properties of mesoporous silicates are dependent on the specific synthetic procedures used in their manufacture [53]. Therefore, to ensure comparability and relevance to templating methods used in many biotechnology applications of mesoporous silicates [1–21,23–30,32,33,35–40,43,44,46,47], the particles examined in this study are synthesised via the same methods. We have produced these mesoporous silicates in particle sizes ~ 150 nm, ~ 800 nm and ~ 4 μm and pore sizes of 3 nm, 7 nm and 16 nm respectively, synthesised with cationic and neutral surfactants. We examine their suitability for drug delivery from a toxicological standpoint, using both *in vitro* and *in vivo* measures.

Materials and Methods

Materials

Tetraethoxysilane (TEOS), cetyltrimethylammonium bromide (CTAB), ethanol, methanol, hydrochloric acid (37%), sodium hydroxide, sodium chloride, potassium chloride, magnesium sulphate, calcium chloride, trimethylbenzene (TMB), human insulin, hydrocortisone, carboxymethylcellulose (medium viscosity) and glutaraldehyde were all obtained from Sigma. Pluronic P123 ($\text{EO}_{20}\text{PO}_{70}\text{EO}_{20}$), was obtained from BASF (Badische Anilin- & Soda-Fabrik). Growth factor, fetal bovine serum, trypsin, DMEM, Medium 199, penicillin/streptomycin and phosphate buffered saline (PBS) were all obtained from Invitrogen. MTT cell assay kits were

obtained from Promega. An endotoxin assay kit was obtained from Cambrex Bioscience Walkersville.

Mesoporous silicate (MPS) syntheses

MCM-41 [36], SBA-15 [54] and MCF [52] were synthesised according to previously published protocols. The surfactant was removed from MCM-41 by three different methods – refluxing with acidified methanol (1.5 g of 9 ml of HCl (37 %) in 160 ml of methanol) followed by washing with methanol, Soxhlet extraction in ethanol for 24 hours or calcination in flowing air (550°C for 6 hours). The surfactant P123 was removed from SBA-15 and MCF by Soxhlet extraction in ethanol for 24 hours. All materials were heated under vacuum at 60°C to remove any residual ethanol/methanol before use for in vitro or in vivo studies.

MPS characterisation

FTIR spectra were obtained with a potassium bromide (KBr) disc of each mesoporous particle. Elemental analysis was performed to determine the percentage of carbon, hydrogen and nitrogen on each particle using a CHN analyser (PE-2400II; Perkin-Elmer). Nitrogen gas adsorption/desorption isotherms were measured at 77 K using a Micromeritics ASAP 2010 system. Samples were pretreated by heating under vacuum at 348 K for 12 h. The surface area was measured using the Brunauer-Emmett-Teller (BET) method [55]. The pore size data were analyzed by the thermodynamic-based Barrett-Joyner-Halenda (BJH) method [56] on the adsorption and desorption branches of the N₂ isotherm. Particle size was measured using a ZetaPALS (Brookhaven Instruments Corporation) and a Multisizer 3 Coulter counter (Beckman Coulter). Samples were pretreated by sonication and vortexing for 2 hours. Transmission electron microscopy was conducted using a JEOL JEM 200CX or a JEOL JEM 2010 electron microscope operated at an accelerating voltage of 200 kV. The powder was suspended in ethanol and placed directly on a carbon-coated copper grid. Scanning electron microscopy was conducted using a FEI/Philips XL30 FEG ESEM. Samples were dried and ground before SEM analysis. SEM images were analysed using Gatan Digital Micrograph Version 3.6.5. Powder X-ray diffraction data was obtained on a Philips X'pert diffractometer using Ni filtered Cu KR radiation with $\lambda=1.54 \text{ \AA}$. Samples were analyzed from 0.3° to 70° 2 θ . An endotoxin assay was conducted using the QCL-1000® test kit from Cambrex – samples were mixed with the LAL reagent and chromogenic substrate reagent over a short incubation period (16 minutes), and the absorbance was read at 408 nm.

In vitro cell assays

In vitro cell viability in the presence of mesoporous silicates were investigated by MTT and live/dead cytotoxicity assays using human mesothelial cells line (ATCC, MeT-5a), mouse peritoneal macrophage cells (ATCC, PMJ2-PC) and mouse myoblast cells, differentiated into muscle cells (ATCC, C2C12). MPS in media without cells were tested and found not to interfere with the MTT assay. Human mesothelial cells were cultured in Medium 199, containing Earle's salts, L-glutamine and 2.2 g/L sodium bicarbonate and supplemented with 3.3 nM epidermal growth factor, 400 nM hydrocortisone, 870 nM insulin, 20 mM HEPES, 1% penicillin/streptomycin and 10% fetal bovine serum. Peritoneal macrophages were cultured in DMEM medium (GIBCO DMEM 11695-010) containing 1% penicillin/streptomycin and 10% fetal bovine serum. Myoblasts were cultured and grown in the same media as macrophages but were differentiated into muscle cells using DMEM with 2% horse serum and 1% penicillin/streptomycin for 8 days, changing the media every 3–4 days. Cells from passages 5 through 25 were used. Cells were seeded into 24 well plates at a density of 50,000 (mesothelial), 25,000 (macrophage) and 30,000 (myoblast) cells per well. On the eighth day after plating myoblasts and after overnight incubation of mesothelials and macrophages, 100 μ l of MPS suspended in PBS at different concentrations was added to each well. Control wells received 100 μ l of PBS.

The MPS were sterilised by UV irradiation for 2 hours and were suspended in sterile PBS at concentrations of 1.1, 3.3 and 5.5 mg/ml and sonicated in a Branson 1510 sonicator bath (Branson Ultrasonics Corp., Danbury, Connecticut) for 2 hours before addition to the cells. After varying incubation periods, cell viability was assayed either by MTT or live/dead assays. Results were reported as means and standard deviations of the measured absorbance normalised to the absorbance of the control cells for the MTT assay.

In vivo studies

All the animals were cared for in compliance with protocols approved by the Animal Care and Use Committee at the Massachusetts Institute of Technology, and the Principles of Laboratory Animal Care (NIH publication #85-23, revised 1985). Young adult male Sprague-Dawley rats weighing 300–400 g and SV129 mice weighing 25 g were purchased from Charles River Labs (Wilmington, MA) and housed in groups in a 6 AM-6 PM light dark cycle. Mesoporous silicates and carboxymethylcellulose were sterilized by UV irradiation for 2 hours.

Carboxymethylcellulose (CMC) was dissolved in sterile phosphate buffered saline (1% w/v). MPS particles were suspended in 1% CMC and sonicated for 2 hours before being loaded into 1 ml syringes under sterile conditions. Anaesthesia was induced briefly, prior to injection, with isofluroane in 100% oxygen. Each rat received one subcutaneous injection of 30 mg in 1 ml of 1% CMC and one intramuscular injection into the sciatic nerve region of 30 mg in 0.6 ml of 1% CMC. Mice received either one subcutaneous injection or one intraperitoneal injection of MPS suspended in 1 ml of 1% CMC. Intraperitoneal injections of 1% CMC and the filtrate from 30 mg/ml 1% CMC after sonication for 2 hours were also given to mice as controls. Tissues recovered from the necropsy were fixed in 10% formalin, embedded in paraffin, sectioned, and stained with hematoxylin and eosin for histological examination using standard techniques. Gram staining of fluid from mice peritoneum was also conducted. Intravenous injections of the smallest mesoporous silica particles (MCM-41_{ref}) suspended in PBS were conducted through the mouse tail vein. The volume injected was 0.3 mls of an MCM-41_{ref} suspension (20 mg/ml) and PBS (0.3 ml) was injected as a control.

Statistics

All comparisons were done with a t-test assuming unequal variance using SPSS 12.0 (SPSS Inc., Chicago, IL). A p value < 0.05 was considered statistically significant. We corrected for multiple comparisons by dividing the p value by the number of comparisons (i.e the Bonferroni correction).

Results

Characterization of mesoporous silicates

Three types of unfunctionalized mesoporous silicates, MCM-41, SBA-15 and MCF, were synthesized for this study (Table 1). The three types differ greatly in the degree of order of their pore structure, pore and particle sizes and were synthesised with two different surfactants. SBA-15 and MCF were prepared with a neutral block co-polymer ethylene oxide-propylene oxide-ethylene oxide (P123). FTIR studies showed no P123 surfactant present in SBA-15 and MCF after removal by Soxhlet extraction (repeated refluxing) in ethanol (Figure 1a). MCM-41 was prepared with the cationic surfactant CTAB which is more difficult to remove after synthesis. Soxhlet extraction in ethanol did not remove CTAB fully. Refluxing in acidified methanol (MCM-41_{ref}) or heating gradually to 550 degrees Celsius under the flow of air (calcining, MCM-41_{cal}) removed much more of the cationic surfactant, as indicated by FTIR (Figure 1b). All 4 MPS (MCM-41_{ref}, MCM-41_{cal}, SBA-15 and MCF) have identical FTIR spectra and each peak is identifiable with a vibration in mesoporous silica particles, i.e. O-Si-O bending band ~ 480 cm⁻¹, Si-O bending ~ 800cm⁻¹, SiOH bending ~950 cm⁻¹, Si-O-Si ~ 1000–1200 cm⁻¹ and SiOH stretching band ~ 3500 cm⁻¹. Elemental analysis indicated that

very low amounts of carbon and hydrogen and no nitrogen were present in all 4 samples (Table 1). An endotoxin assay showed that there was no detectable gram negative endotoxin on any of the four particle types at a concentration of 1 mg/ml, (the detection limit was less than 0.1 EU/ml).

The large surface areas and different pore sizes of the chosen MPS are presented in Table 1. The ordered mesoporous structure of all three materials is clearly observed from the sharp step in the nitrogen adsorption/desorption isotherm due to the capillary condensation/evaporation of the nitrogen gas in the mesopores at different relative pressures, dependent on the pore size (Figure 2a). MCM-41 had the smallest sized channels and pore openings (~ 3 nm) while MCF, a mesocellular foam, had much larger pores. MCF was more disordered, consisting more of cell-like structures (40 nm wide) with narrow openings (16 nm) as calculated from the adsorption and desorption branches of the isotherm respectively. SBA-15 and MCM-41 both had hexagonally highly ordered straight channel pores, as illustrated by the low angle XRD spectra in Figure 2b and in the TEM images in Figure 3. The unit cell parameters (a) of the three hexagonally ordered materials are listed in Table 1. The particle sizes of the three materials are given in Table 2 and can be seen in the SEM images in Figure 3. MCM-41 and SBA-15 consisted of regularly ordered spheres (100 – 150 nm) and rods (700 – 800 nm) respectively, while MCF particles were much larger (~ 4 µm) with a more irregular morphology. MCM-41 had similar physical characteristics whether refluxed or calcined, i.e. particle size, morphology and pore size, although MCM-41_{ref} had a lower surface area than MCM-41_{cal}, as calculated by the BET theory [55].

Some aggregation was observed as evidenced by the difference in the particle sizes measured by SEM compared to those measured in phosphate buffered saline after sonication and vortexing (the usual preparation of the materials for cytotoxicity and *in vivo* experiments) using ZetaPALS and Coulter counter size analysers (Table 2). Particle sizing, TEM and SEM analyses showed that the particle sizes were not changed by UV sterilization, sonication for 2 hours and incubation for 4 days in PBS at 37°C (not shown), showing that particles would be stable in the conditions used *in vitro*.

Cytotoxicity of materials

Human mesothelial cells, mouse peritoneal macrophages and mouse myoblasts differentiated into muscle cells were exposed to varying amounts of mesoporous silicates (Figure 4–Figure 6). MCM-41_{soxhleted} was very toxic to all cell lines examined (not shown) at all concentrations and time points, (0.1, 0.3 and 0.5 mg/ml and 24, 72 and 96 hours). Consequently, MCM-41_{soxhleted} was not used in subsequent studies. In general the toxicity of MCM-41_{cal}, SBA-15 and MCF to mesothelial cells and myoblasts increased with the concentration of particles, most significantly with the mesothelial cell line. Macrophages showed little or no toxicity from those three particle types, Figure 4. MCM-41_{ref} was more toxic to the macrophages ($p < 0.0001$ for 0.5 mg/ml at 4 days, compared to all other MPS) (Figure 4) and exhibited a lower toxicity to the mesothelial cell line ($p < 0.0001$ for 0.5 mg/ml at 4 days, compared to all other MPS, Figure 5). In order to verify that cytotoxicity was not due to particles landing on top of the cells and inhibiting nutrient or oxygen uptake, the mesothelial cell viability experiments were repeated with the particles added before the cells had been plated; the results were identical. To assess whether toxicity was due to the particles themselves, or a soluble factor that was released, 5.5 mg of SBA-15 per ml of mesothelial medium were sonicated and vortexed for 2 hours and incubated at 37°C for 4 days. TEM and SEM imaging indicated that the particle size and mesoporous structure were unchanged. The pH of the medium was also found to be unchanged after this treatment. Subsequently, mesothelial cells were incubated for four days with either the SBA-15 supernatant or the particles. The SBA-15 supernatant did

not affect cell viability while the SBA-15 particle suspension (0.5 mg/ml) killed 50% of cells present.

In vivo studies

In vivo experiments were carried out using 1% carboxymethylcellulose as a carrier, unless otherwise stated, due to the tendency of the larger MPS to fall out of suspension. Particles were injected subcutaneously and at the sciatic nerve in rats; the latter location was selected because of the close proximity of many different tissue types (nerve, muscle, blood vessels, connective tissue). MCM-41_{cal}, MCM-41_{ref}, SBA-15 and MCF were injected at a concentration of 50 mg/ml at the sciatic nerve. The same animal was injected with 1 ml of the same suspension at a concentration of 30 mg/ml subcutaneously on the contralateral limb. At predetermined time points (Table 3), rats were sacrificed for necropsy. One rat injected with MCM-41_{cal} particles developed difficulty moving its hind limbs on the second day after injection and was euthanized, and one injected with MCM-41_{ref} particles died 3 days after injection. All other rats (n = 40) injected with mesoporous silicates did not exhibit any overt toxicity, including gait abnormalities on the side where the sciatic nerve injections were performed.

Grossly, MPS materials disappeared from the sciatic nerve region much faster than from the subcutaneous depot, i.e. in general much smaller amounts of all four MPS were recovered. At early time points, quite large deposits of material were found subcutaneously (Figure 7a–c). Irrespective of the site of injection, very small amounts or no MPS materials were observed at the two and three month points (Figure 7d–f). In many cases, MPS were detected on histological assessment of tissues at two and three months, even though no or very small amounts of MPS were observed on gross dissection, Figure 8.

Similar histologic observations were made with all four particle types. There was an inflammatory reaction to the particles which decreased substantially from the 4 day to the 3 month time points. There was no significant injury to surrounding tissues (muscle, nerve, blood vessels). At the 4 day time point, the inflammation consisted predominantly of neutrophils with some macrophages. The inflammation decreased over time and became dominated by mononuclear cells such as lymphocytes and macrophages. The surrounding tissue showed evidence of healing, with granulation tissue formation and mild fibrosis over time. The spleens of all the rats injected were without focal lesions on gross dissection. Histologically, there was expansion of the red pulp, predominantly by foamy macrophages, noticeable at the earlier time point of 4 days for the nanoparticles (MCM-41) and at two weeks for the larger microparticles (MCF). The spleens exhibited progressively less red pulp expansion over the 3 month time course of the experiments.

To assess the applicability of MPS for intraperitoneal use, particles were injected into SV129 mice (Table 4), a model we selected because of our extensive experience with it for testing intraperitoneal drug delivery [50]. All mice appeared healthy at 5 hours after IP injection of all doses assessed here. Mice that received intraperitoneal injections of 30 mg of mesoporous silicates of all sizes either died or became sufficiently distressed within 24 hours that they were euthanized. To find the upper limit of the non-lethal dosage range, we injected animals with decreasing doses of SBA-15 (Figure 9), which had been uniformly fatal at 30 mg. Mice injected with 10 mg or 5 mg of SBA-15 that needed to be euthanized became ill 30–40 hours after injection. Doses of 1 mg or less were non-fatal. On necropsy, the viscera of the spontaneously deceased and euthanized animals had a glistening quality, but there was no obvious injury, hemorrhage or other catastrophic pathology. Histologic evaluation of the peritoneal cavity revealed reactive mesothelial cells with only mild acute and chronic inflammation and no evidence of necrosis of the underlying abdominal wall musculature (Figure 10).

To elucidate the cause of death of the animals injected with intraperitoneal MPS, samples of peritoneal fluid from the surface of the viscera of the deceased or euthanized animals were examined microscopically. Gram staining did not reveal bacteria, and hematoxylin-eosin staining showed only occasional white blood cells, suggesting the absence of a massive inflammatory process (i.e. peritonitis) and correlating with the histologic evaluation. To address the possibility that toxicity was due to the release of a toxic soluble factor, 2 groups of MPS (MCM-41_{ref} and SBA-15) were sonicated and vortexed for 2 hours and the supernatants (filtered through a 0.2 μm sterile filter) was injected intraperitoneally. There were no detectable sequelae. Similarly, injection of the carrier for all intraperitoneal injections, 1% CMC, did not cause toxicity (Table 4).

Our hypothesis regarding the difference in toxicity between the rat and murine data was that this was due to a combination of a large difference in dose/weight (0.17 g/kg and 1.2 g/kg respectively), and pharmacokinetics (intraperitoneal delivery of a toxic material is likely to result in more rapid systemic distribution, and therefore toxicity, than subcutaneous injection). The greater toxicity of MPS to mesothelial cells than to other cells (Figure 5) raised the possibility that peritoneal injury was the cause of death. However, intravenous injection of MPS (Table 4) uniformly resulted in rapid death, suggesting that the toxicity was not peritoneal in origin (as did the benign peritoneal histology). The view that pharmacokinetics played a significant role was bolstered by the fact that mice injected with 30 mg of MPS (Table 4) subcutaneously did not experience detectable toxicity. The MPS appeared to have the same generally benign local biocompatibility seen with subcutaneous injections in rats: two months after injection in mice, small quantities of SBA-15 and only trace MCM-41 were found. Light microscopy of the lungs from animals that received MPS intravenously or at high doses intraperitoneally revealed blood clots reflecting either *in situ* thrombi or emboli in the pulmonary arteries, arterioles and capillaries. The lungs of the animals injected with the carrier (1% CMC) or low doses of MPS subcutaneously did not have these clots and appeared normal (Figure 11).

Discussion

All three materials, MCM-41, SBA-15 and MCF have been suggested in the literature for use as drug delivery systems, and as formulated here have the mesoporous structure advocated in the literature to release adsorbed drugs in a controlled manner [1,3,19]. While tissue biocompatibility for all particles was adequate, or at least comparable to that seen with many other particle types when delivered in large quantities [50], the systemic toxicity was much worse than that of more commonly used polymeric delivery systems. Thirty mg of intraperitoneally injected silicates invariably resulted in death or distress necessitating euthanasia; in contrast, even 100 mg of poly(lactic-co-glycolic) acid (PLGA) microspheres caused no detectable toxicity in mice of the same strain and mass [50]. Since an absence of lethality was only found at a dose of 1 mg per animal, the silicates tested here would appear to be at least 100 times more lethal than PLGA. We also note the experimental design used here could not detect more subtle forms of toxicity. These findings do not mean that mesoporous silicates cannot or should not be used for drug delivery. However, given the above it would appear prudent to use other systems unless the mesoporous silicates can be shown to be vastly superior in terms of their release or targeting properties. This would be particularly true if large quantities of particle are to be used. It is also possible that the toxicity of the mesoporous silicates could be mitigated by surface adsorption of proteins, functional groups or polymers [20,51]. Blumen et al [7] indicated that pegylated mesoporous silicates were non-toxic in peripheral lung tissue. Such pegylation or other coating strategies may also reduce toxicity systemically.

All three particle types showed varying degrees of cytotoxicity *in vitro*. Soxhleted MCM-41 was extremely cytotoxic to all three cell lines, presumably due to the residual cationic surfactant present in its pores. The toxicity of the MPS was due to interaction with the particles themselves, rather than with a product of particle degradation, as shown by the 100% cell survival in the experiments where cells were exposed to particle-free supernatants from a suspension of SBA-15. Toxicity to mesothelial cells and C2C12 cells was also not likely to be due to impairment of diffusion of oxygen and nutrients since it made no difference to cell survival whether the particles were added before or after (i.e. on top of) the cells were plated. Cell death increased with duration of exposure. In general, MCM-41_{ref} was less toxic to mesothelial cells but slightly more toxic to macrophages than the other particles. Overall, the MPS toxicity to mesothelial and C2C12 cell lines (and macrophages with MCM-41_{ref}) appeared to be dose dependent and exhibited time dependence with the mesothelial cell line. Particle size (or mesoporous structure) had no bearing on the *in vitro* cytotoxicity of mesoporous silicates, within the range of particle sizes examined here (150 – 4000 nm).

In all particle groups, there were still MPS particles present both in the sciatic nerve region and subcutaneously at up to 3 months, and the rate of decrease in size of the subcutaneous nodules was grossly similar for all 4 particle types and sizes. The amount of residue remaining was particularly difficult to assess in the sciatic nerve region, but histology revealed its presence for up to 3 months. The inflammatory response *in vivo* was comparable to PLGA [50], a biomaterial commonly used in drug delivery. Particle size (in the range studied, 150 nm – 4 µm) did not appear to affect biocompatibility although the two rats that became ill both were injected with the smaller (150 nm) MCM-41 particles. The destination of the particles as the subcutaneous nodule decreases in size was not determined but subtle changes in the architecture of the spleens of the rats were observed at earlier time points for the smaller particles (4 days) and later time points (2 weeks) for the larger particles. This suggests that the smaller particles (MCM-41) reached the spleen faster than the larger particles, in particular MCF. After 2 or 3 months the spleens had regained their normal architecture.

Mice injected with all 4 types of MPS particles intraperitoneally died or were euthanized within 24 hours of injection at doses of 30 mg. The non-fatal dose was below 5 mg. MCM-41 particles were toxic intraperitoneally, whether the porous particles were extracted by calcination (heating to 550°C) or refluxing in acidified methanol, indicating that the toxicity is due to the particles themselves. This is confirmed by the fact that supernatants in which the particles were incubated were not detectably toxic. Our efforts to establish the cause of the toxicity suggested that endotoxin (negative assay), bacterial infection (negative Gram stain), and/or peritonitis (absence of inflammatory cells) were unlikely causes, and intravenous toxicity demonstrated that this toxicity did not originate in the peritoneum. The higher death rate in animals injected in the peritoneum compared to subcutaneously may be due to the faster rate of clearance of the silica particles from the former site, resulting in a higher systemic dose of the mesoporous particles. It is possible, given the rapidity of death and the findings on necropsy, that pulmonary embolism and/or thrombosis were the cause of death. While the etiology of the pulmonary clots is not clear, it bears mentioning that colloidal silica is pro-thrombotic [57] and that amorphous silica can cause complement activations [8]. The role of these mechanisms, if any, in the pathogenesis of our observations is unclear.

Conclusions

Unfunctionalised mesoporous silicates of particles sizes 150 nm – 4000 nm exhibit benign local biocompatibility but considerable systemic toxicity. This toxicity appears to result from the particles themselves and not from any contaminants or degradation products. These findings suggest that biomedical applications of mesoporous silicates should be explored in the context of modifications to reduce toxicity.

Acknowledgements

This work was supported by MCOIF-CT2007-040150 (to SH), NIH EB000244 (to RL) and NIH GM073626 (to DSK). Simon White and David Bennis are acknowledged for running the nitrogen adsorption analyses at the MSSSI, University of Limerick.

References

1. Lai CY, Trewyn BG, Jeftinija DM, Jeftinija K, Xu S, Jeftinija S, et al. A mesoporous silica nanosphere-based carrier system with chemically removable CdS nanoparticle caps for stimuli-responsive controlled release of neurotransmitters and drug molecules. *J Am Chem Soc* 2003;125(15):4451–4459. [PubMed: 12683815]
2. Lopez T, Basaldella EI, Ojeda ML, Manjarrez J, Alexander-Katz R. Encapsulation of valproic acid and sodic phenytoin in ordered mesoporous SiO₂ solids for the treatment of temporal lobe epilepsy. *Opt Mater* 2006;29(1):75–81.
3. Yang Q, Wang SH, Fan PW, Wang LF, Di Y, Lin KF, et al. pH-responsive carrier system based on carboxylic acid modified mesoporous silica and polyelectrolyte for drug delivery. *Chem Mater* 2005;17(24):5999–6003.
4. Zhu YF, Shi JL, Li YS, Chen HR, Shen WH, Dong XP. Hollow mesoporous spheres with cubic pore network as a potential carrier for drug storage and its in vitro release kinetics. *J Mater Res* 2005;20(1):54–61.
5. Tang Q, Xu Y, Wu D, Sun Y. A study of carboxylic-modified mesoporous silica in controlled delivery for drug famotidine. *Journal of Solid State Chemistry* 2006;179:1513–1520.
6. Vallet-Regi M, Ramila A, del Real RP, Perez-Pariente J. A new property of MCM-41: Drug delivery system. *Chem Mater* 2001;13(2):308–311.
7. Vallet-Regi M, Doadrio JC, Doadrio AL, Izquierdo-Barba I, Perez-Pariente J. Hexagonal ordered mesoporous material as a matrix for the controlled release of amoxicillin. *Solid State Ionics* 2004;172(1–4):435–439.
8. Fagundes LB, Sousa TGF, Sousa A, Silva VV, Sousa EMB. SBA-15-collagen hybrid material for drug delivery applications. *J Non-Cryst Solids* 2006;352(32–35):3496–3501.
9. Kim HJ, Matsuda H, Zhou HS, Honma I. Ultrasound-triggered smart drug release from a poly (dimethylsiloxane)-mesoporous silica composite. *Adv Mater* 2006;18(23):3083–+
10. Mellaerts R, Aerts CA, Van Humbeek J, Augustijns P, Van den Mooter G, Martens JA. Enhanced release of itraconazole from ordered mesoporous SBA-15 silica materials. *Chem Commun* 2007; (13):1375–1377.
11. Heikkila T, Salonen J, Tuura J, Hamdy MS, Mul G, Kumar N, et al. Mesoporous silica material TUD-1 as a drug delivery system. *Int J Pharm* 2007;331(1):133–138. [PubMed: 17046183]
12. Li X, Zhang LX, Dong XP, Liang J, Shi JL. Preparation of mesoporous calcium doped silica spheres with narrow size dispersion and their drug loading and degradation behavior. *Micropor Mesopor Mat* 2007;102(1–3):151–158.
13. Yang PP, Huang SS, Kong DY, Lin J, Fu HG. Luminescence functionalization of SBA-15 by YVO₄ : Eu³⁺ as a novel drug delivery system. *Inorg Chem* 2007;46(8):3203–3211. [PubMed: 17371013]
14. Wu ZJ, Jiang Y, Kim TH, Lee KT. Effects of surface coating on the controlled release of vitamin B, from mesoporous silica tablets. *J Control Release* 2007;119(2):215–221. [PubMed: 17434225]
15. Son YH, Park M, Bin Choy Y, Choi HR, Kim DS, Park KC, et al. One-pot synthetic route to polymer-silica assembled capsule encased with nonionic drug molecule. *Chem Commun* 2007;(27):2799–2801.
16. Nunes CD, Vaz PD, Fernandes AC, Ferreira P, Romao CC, Calhorda MJ. Loading and delivery of sertraline using inorganic micro and mesoporous materials. *Eur J Pharm Biopharm* 2007;66(3):357–365. [PubMed: 17240126]
17. Lu J, Liong M, Zink JI, Tamanoi F. Mesoporous silica nanoparticles as a delivery system for hydrophobic anticancer drugs. *Small* 2007;3(8):1341–1346. [PubMed: 17566138]

18. Ruiz-Hernandez E, Lopez-Noriega A, Arcos D, Izquierdo-Barba I, Terasaki O, Vallet-Regi M. Aerosol-assisted synthesis of magnetic mesoporous silica spheres for drug targeting. *Chem Mater* 2007;19(14):3455–3463.
19. Zhou ZY, Zhu SM, Zhang D. Grafting of thermo-responsive polymer inside mesoporous silica with large pore size using ATRP and investigation of its use in drug release. *J Mater Chem* 2007;17(23):2428–2433.
20. Song SW, Hidajat K, Kawi S. pH-controllable drug release using hydrogel encapsulated mesoporous silica. *Chem Commun* 2007;(42):4396–4398.
21. Zeng W, Qian XF, Yin J, Zhu ZK. The drug delivery system of MCM-41 materials via co-condensation synthesis. *Mater Chem Phys* 2006;97(2–3):437–441.
22. Linnell T, Riikonen J, Salonen J, Kaukonen AM, Laitinen L, Hirvonen J, et al. Surface chemistry and pore size affect carrier properties of mesoporous silicon microparticles. *Int J Pharm* 2007;343(1–2):141–147. [PubMed: 17600644]
23. Vallet-Regi M, Balas F, Arcos D. Mesoporous materials for drug delivery. *Angew Chem Int Edit* 2007;46(40):7548–7558.
24. Vallhov H, Gabrielsson S, Stromme M, Scheynius A, Garcia-Bennett AE. Mesoporous silica particles induce size dependent effects on human dendritic cells. *Nano Lett* 2007;7(12):3576–3582. [PubMed: 17975942]
25. Barbe C, Bartlett J, Kong LG, Finnie K, Lin HQ, Larkin M, et al. Silica particles: A novel drug-delivery system. *Adv Mater* 2004;16(21):1959–1966.
26. Carino IS, Pasqua L, Testa F, Aiello R, Puoci F, Iemma F, et al. Silica-based mesoporous materials as drug delivery system for methotrexate release. *Drug Deliv* 2007;14(8):491–495. [PubMed: 18027178]
27. Clifford NW, Iyer KS, Raston CL. Encapsulation and controlled release of nutraceuticals using mesoporous silica capsules. *J Mater Chem* 2008;18(2):162–165.
28. Ambrogi V, Perioli L, Marmottini F, Giovagnoli S, Esposito M, Rossi C. Improvement of dissolution rate of piroxicam by inclusion into MCM-41 mesoporous silicate. *Eur J Pharm Sci* 2007;32(3):216–222. [PubMed: 17826966]
29. Manzano M, Aina V, Arean CO, Balas F, Cauda V, Colilla M, et al. Studies on MCM-41 mesoporous silica for drug delivery: Effect of particle morphology and amine functionalization. *Chem Eng J* 2008;137(1):30–37.
30. Pasqua L, Testa F, Aiello R, Cundari S, Nagy JB. Preparation of bifunctional hybrid mesoporous silica potentially useful for drug targeting. *Micropor Mesopor Mat* 2007;103(1–3):166–173.
31. Gu J, Fan W, Shimojima A, Okubo T. Organic-inorganic mesoporous nanocarriers, integrated with biogenic ligands. *Small* 2007;3(10):1740–1744. [PubMed: 17786917]
32. Izquierdo-Barba I, Ruiz-Gonzalez L, Doadrio JC, Gonzalez-Calbet JM, Vallet-Regi M. Tissue regeneration: A new property of mesoporous materials. *Solid State Sci* 2005;7(8):983–989.
33. Izquierdo-Barba I, Martinez A, Doadrio AL, Perez-Pariente J, Vallet-Regi M. Release evaluation of drugs from ordered three-dimensional silica structures. *Eur J Pharm Sci* 2005;26(5):365–373. [PubMed: 16185852]
34. Vallet-Regi M, Izquierdo-Barba I, Ramila A, Perez-Pariente J, Babonneau F, Gonzalez-Calbet JM. Phosphorous-doped MCM-41 as bioactive material. *Solid State Sci* 2005;7(2):233–237.
35. Li X, Shi JL, Zhu YF, Shen WH, Li H, Liang J, et al. A template route to the preparation of mesoporous amorphous calcium silicate with high in vitro bone-forming bioactivity. *J Biomed Mater Res B* 2007;83B(2):431–439.
36. Radu DR, Lai CY, Jeftinija K, Rowe EW, Jeftinija S, Lin VSY. A polyamidoamine dendrimer-capped mesoporous silica nanosphere-based gene transfection reagent. *J Am Chem Soc* 2004;126(41):13216–13217. [PubMed: 15479063]
37. Blumen SR, Cheng K, Ramos-Nino ME, Taatjes DJ, Weiss DJ, Landry CC, et al. Unique uptake of acid-prepared mesoporous spheres by lung epithelial and mesothelioma cells. *Am J Resp Cell Mol* 2007;36(3):333–342.
38. Trewyn BG, Nieweg JA, Zhao Y, Lin VSY. Biocompatible mesoporous silica nanoparticles with different morphologies for animal cell membrane, penetration. *Chem Eng J* 2008;137(1):23–29.

39. Chung TH, Wu SH, Yao M, Lu CW, Lin YS, Hung Y, et al. The effect of surface charge on the uptake and biological function of mesoporous silica nanoparticles 3T3-L1 cells and human mesenchymal stem cells. *Biomaterials* 2007;28(19):2959–2966. [PubMed: 17397919]
40. Lin YS, Tsai CP, Huang HY, Kuo CT, Hung Y, Huang DM, et al. Well-ordered mesoporous silica nanoparticles as cell markers. *Chem Mater* 2005;17(18):4570–4573.
41. Wu SH, Lin YS, Hung Y, Chou YH, Hsu YH, Chang C, et al. Multifunctional mesoporous silica nanoparticles for intracellular labeling and animal magnetic resonance imaging studies. *ChemBiochem* 2008;9(1):53–57. [PubMed: 17999392]
42. Tsai CP, Hung Y, Chou YH, Huang DM, Hsiao JK, Chang C, et al. High-contrast paramagnetic fluorescent mesoporous silica nanorods as a multifunctional cell-imaging probe. *Small* 2008;4(2):186–191. [PubMed: 18205156]
43. Fu Q, Rao GVR, Ista LK, Wu Y, Andrzejewski BP, Sklar LA, et al. Control of molecular transport through stimuli-responsive ordered mesoporous materials. *Adv Mater* 2003;15(15):1262–1266.
44. Park C, Oh K, Lee SC, Kim C. Controlled release of guest molecules from mesoporous silica particles based on a pH-responsive polypseudorotaxane motif. *Angew Chem Int Edit* 2007;46(9):1455–1457.
45. Mal NK, Fujiwara M, Tanaka Y. Photocontrolled reversible release of guest molecules from coumarin-modified mesoporous silica. *Nature* 2003;421(6921):350–353. [PubMed: 12540896]
46. Arruebo M, Galan M, Navascues N, Tellez C, Marquina C, Ibarra MR, et al. Development of magnetic nanostructured silica-based materials as potential vectors for drug-delivery applications. *Chem Mater* 2006;18(7):1911–1919.
47. Roy I, Ohulchanskyy TY, Pudavar HE, Bergy EJ, Oseroff AR, Morgan J, et al. Ceramic-based nanoparticles entrapping water-insoluble photosensitizing anticancer drugs: A novel drug-carrier system for photodynamic therapy. *J Am Chem Soc* 2003;125(26):7860–7865. [PubMed: 12823004]
48. Radin S, El-Bassyouni G, Vresilovic EJ, Schepers E, Ducheyne P. In vivo tissue response to resorbable silica xerogels as controlled-release materials. *Biomaterials* 2005;26(9):1043–1052. [PubMed: 15369693]
49. Castillo J, Curley J, Hotz J, Uezono M, Tigner J, Chasin M, et al. Glucocorticoids prolong rat sciatic nerve blockade in vivo from bupivacaine microspheres. *Anesthesiology* 1996;85(5):1157–1166. [PubMed: 8916834]
50. Kohane DS, Tse JY, Yeo Y, Padera R, Shubina M, Langer R. Biodegradable polymeric microspheres and nanospheres for drug delivery in the peritoneum. *J Biomed Mater Res A* 2006;77A(2):351–361. [PubMed: 16425240]
51. Tomazic-Jezic VJ, Merritt K, Umbreit TH. Significance of the type and the size of biomaterial particles on phagocytosis and tissue distribution. *J Biomed Mater Res* 2001;55(4):523–529. [PubMed: 11288080]
52. Katiyar A, Ji L, Smirniotis P, Pinto NG. Protein adsorption on the mesoporous molecular sieve silicate SBA-15: effects of pH and pore size. *J Chromatogr A* 2005;1069(1):119–126. [PubMed: 15844490]
53. Wan Y, Zhao DY. On the controllable soft-templating approach to mesoporous silicates. *Chem Rev* 2007;107(7):2821–2860. [PubMed: 17580976]
54. Sayari A, Han BH, Yang Y. Simple synthesis route to monodispersed SBA-15 silica rods. *J Am Chem Soc* 2004;126(44):14348–14349. [PubMed: 15521742]
55. Brunauer S, Emmett PHET. Adsorption of gases in multimolecular layers. *J Am Chem Soc* 1938;60:309–319.
56. Barrett EP, Joyner LG, Halenda PP. The determination of pore volume and area distributions in pure substances. *J Am Chem Soc* 1951;73:373–385.
57. Margolis J. The effect of colloidal silica on blood coagulation. *Aust J Exp Biol Med Sci* 1961;39:249–258. [PubMed: 13766692]
58. Governa M, Amati M, Fenoglio I, Valentino M, Coloccini S, Bolognini L, et al. Variability of biological effects of silicas: Different degrees of activation of the fifth component of complement by amorphous silicas. *Toxicol Appl Pharm* 2005;208(1):68–77.

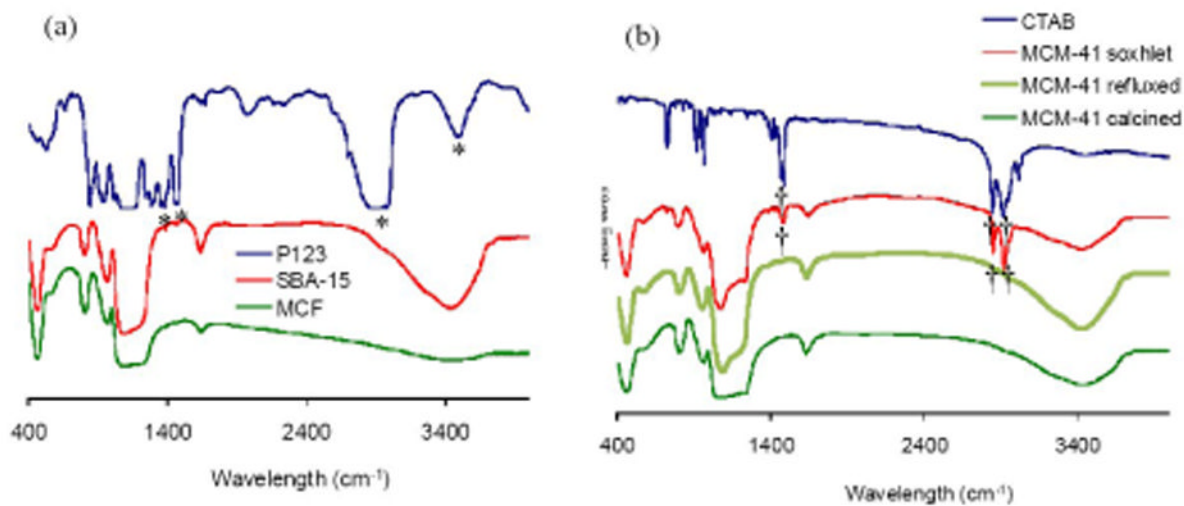


Figure 1. FTIR spectra of (a) P123, SBA-15 and MCF and (b) CTAB and MCM-41 soxhleted, refluxed and calcined. Asterisk (*) indicates the modes of vibration of the P123 surfactant, removed from both SBA-15 and MCF. Dagger (†) indicates the modes of vibration of the CTAB surfactant, still present in MCM-41 soxhleted but removed from MCM-41_{ref} and MCM-41_{cal}.

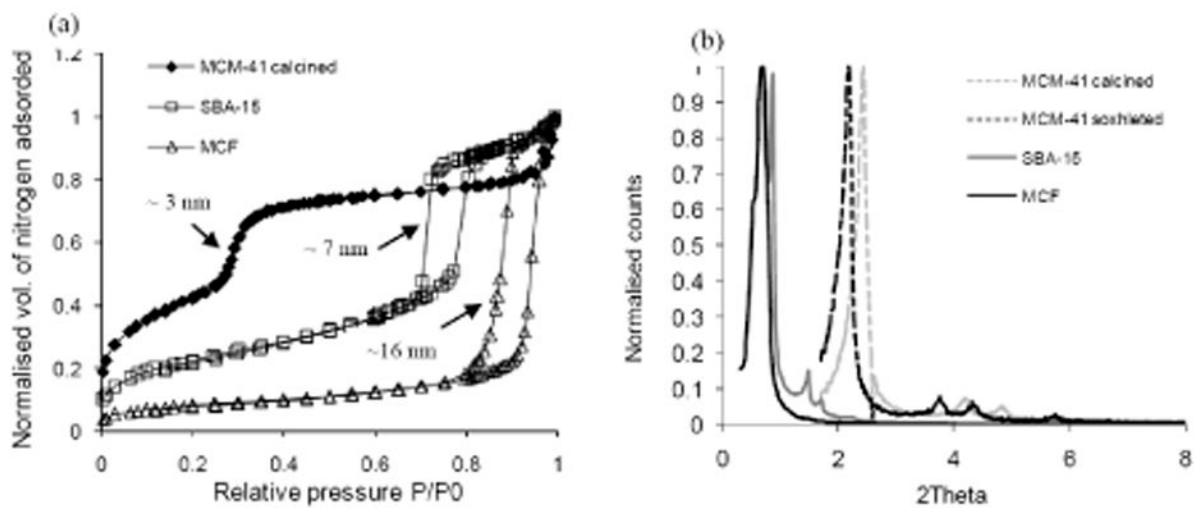


Figure 2.

(a) Nitrogen adsorption isotherms and (b) low angle XRD spectra for MCM-41_{cal}, SBA-15 and MCF. Arrows indicate the width of the pore openings as calculated from the desorption branch of the nitrogen isotherm using BJH theory (see Methods).

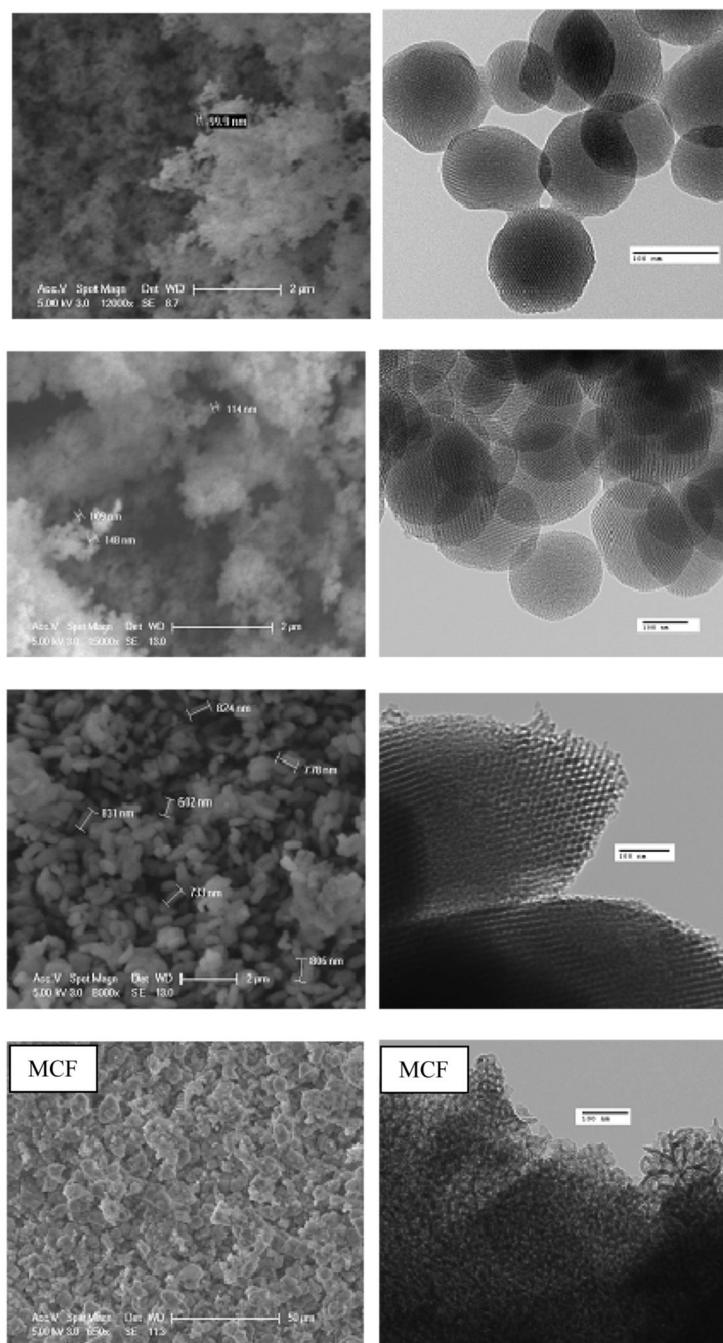


Figure 3. SEM (left) and TEM (right) images of MCM-41_{ref}, MCM-41_{cal}, SBA-15 and MCF.

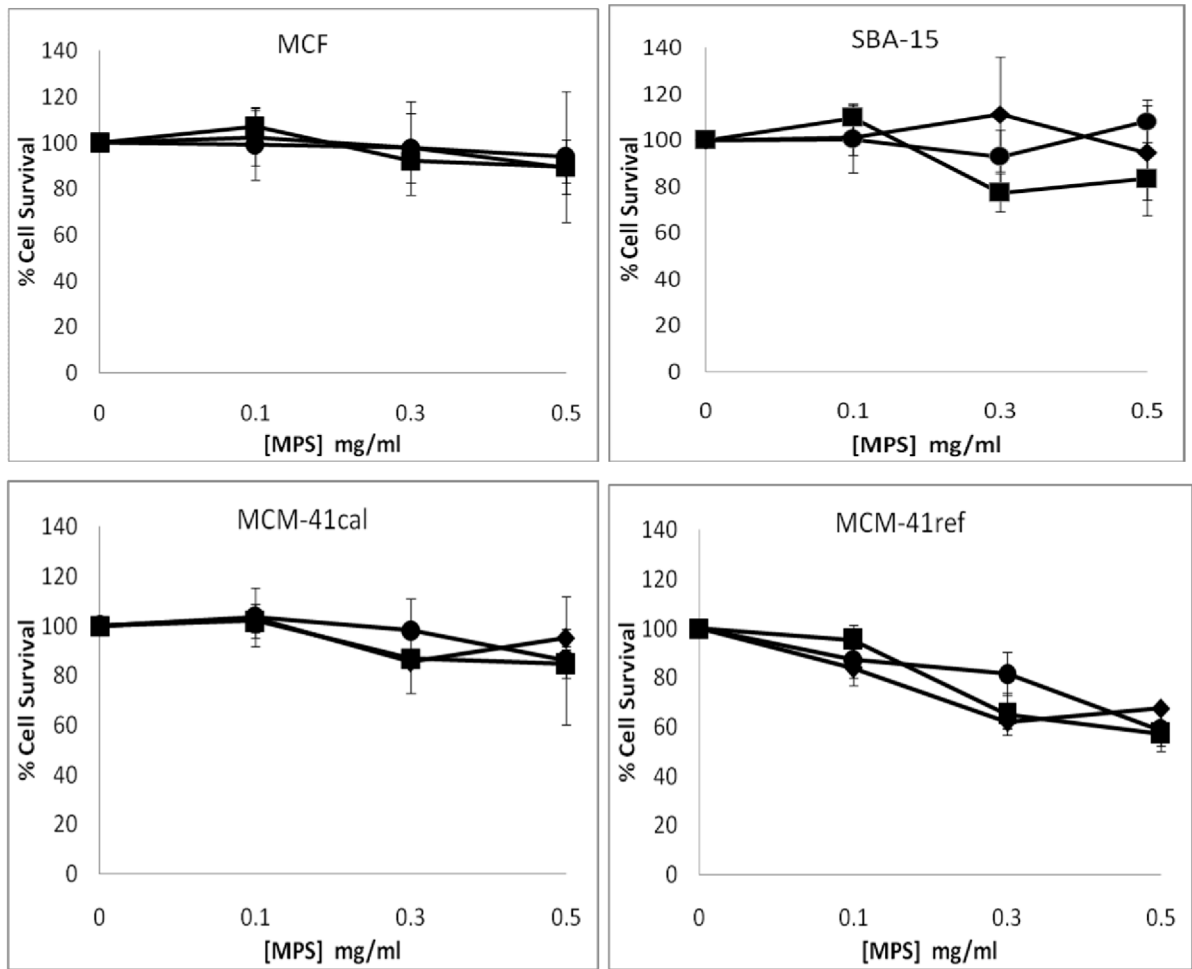


Figure 4. % Cell survival of macrophages upon exposure to MPS for (○) 1 day, (□) 3 days and (◇) 4 days. n = 16 to 24 for individual groups, assessed using an MTT cell viability kit.

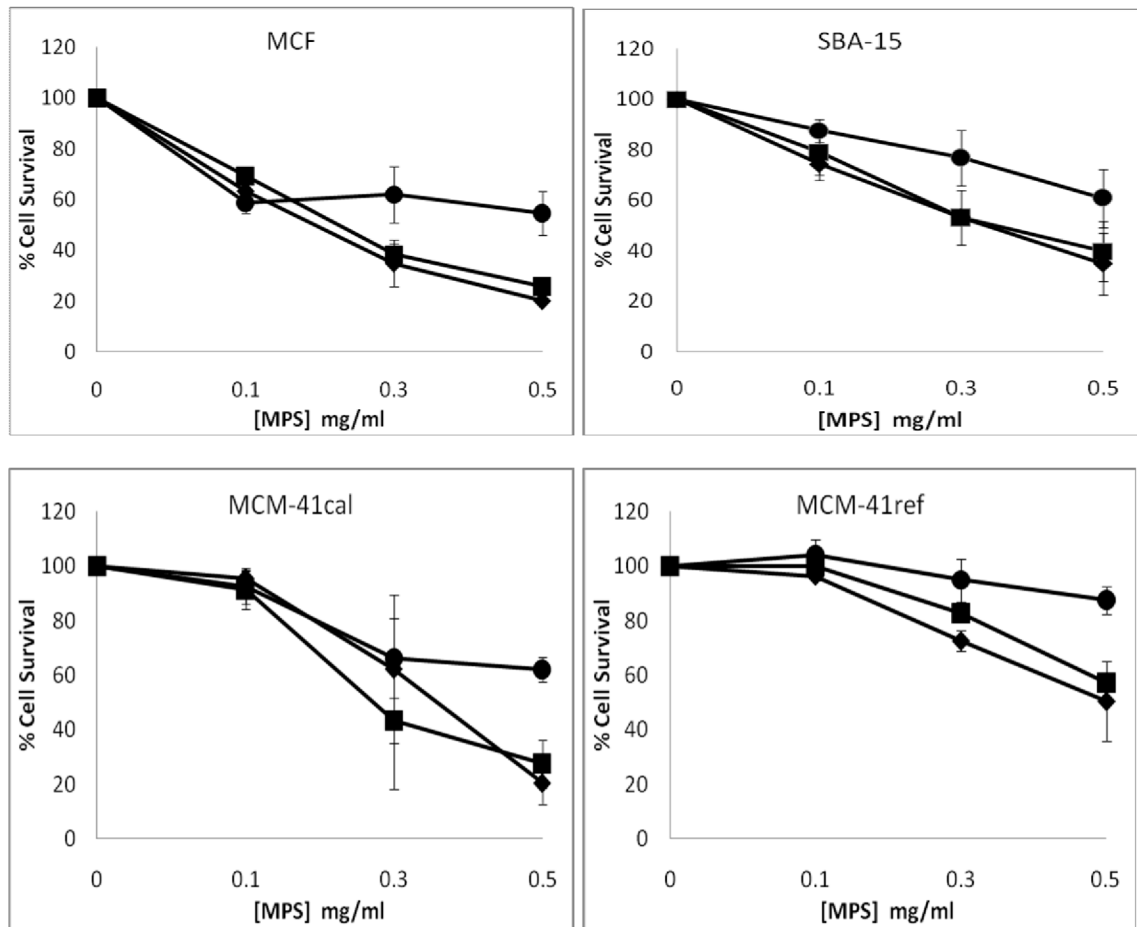


Figure 5. % Cell survival of mesothelial cells upon exposure to MPS for (○) 1 day, (□) 3 days and (◇) 4 days. n = 16 to 24 for individual groups, assessed using an MTT cell viability kit.

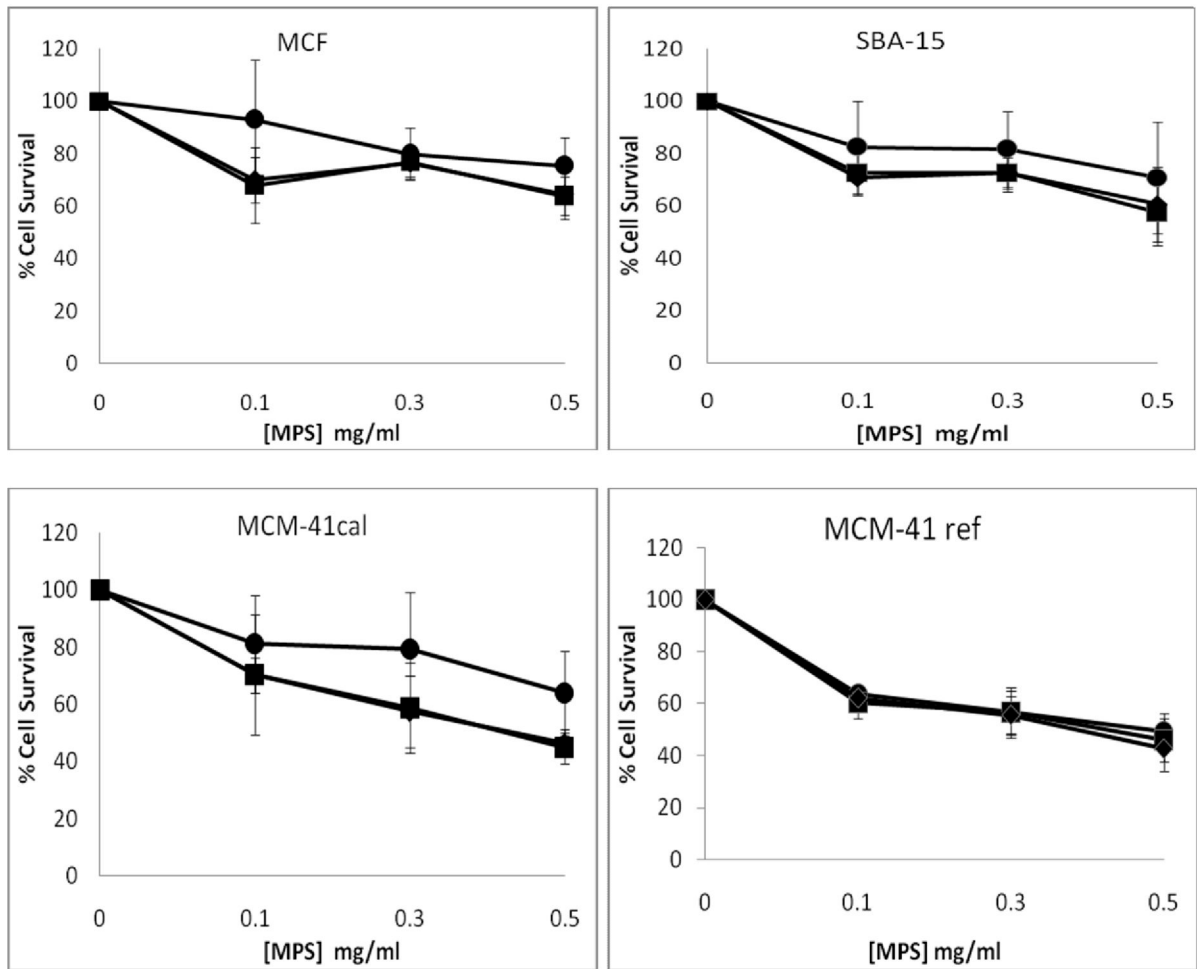


Figure 6. % Cell survival of C2C12 muscle cells upon exposure to MPS for (○) 1 day, (□) 3 days and (◇) 4 days. n = 16 to 24 for individual groups, assessed using an MTT cell viability kit.

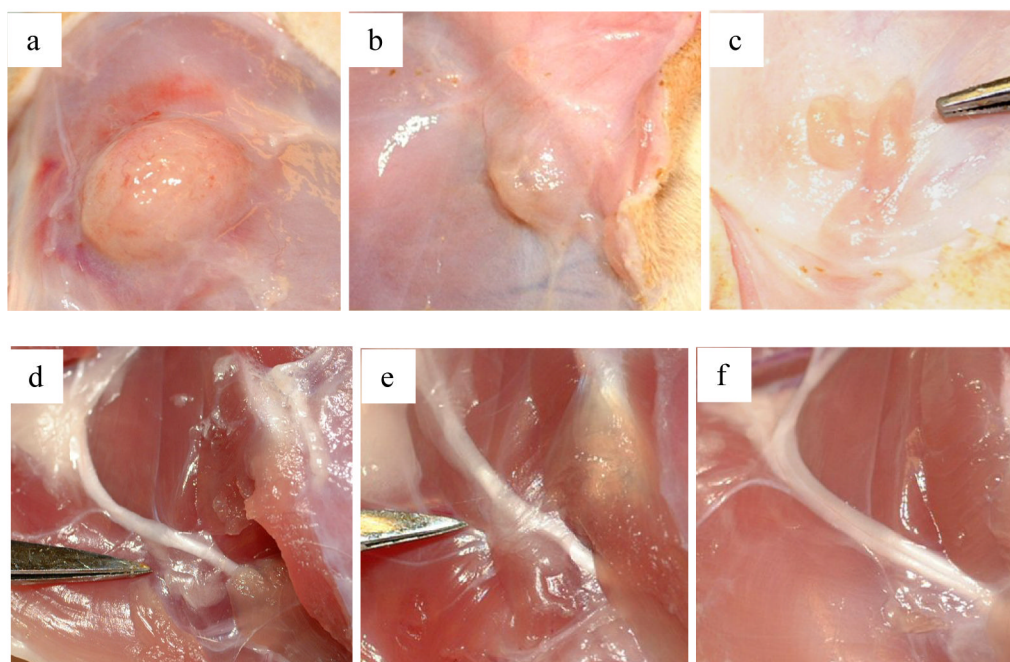


Figure 7. MCF subcutaneous nodule (a) 4 days, (b) 2 weeks and (c) 1 month after injection (30 mg) and (d) MCF, (e) SBA-15 and (f) MCM-41_{cal} 3 months after injection near the sciatic nerve (30 mg). Instruments in the fields indicate residue.

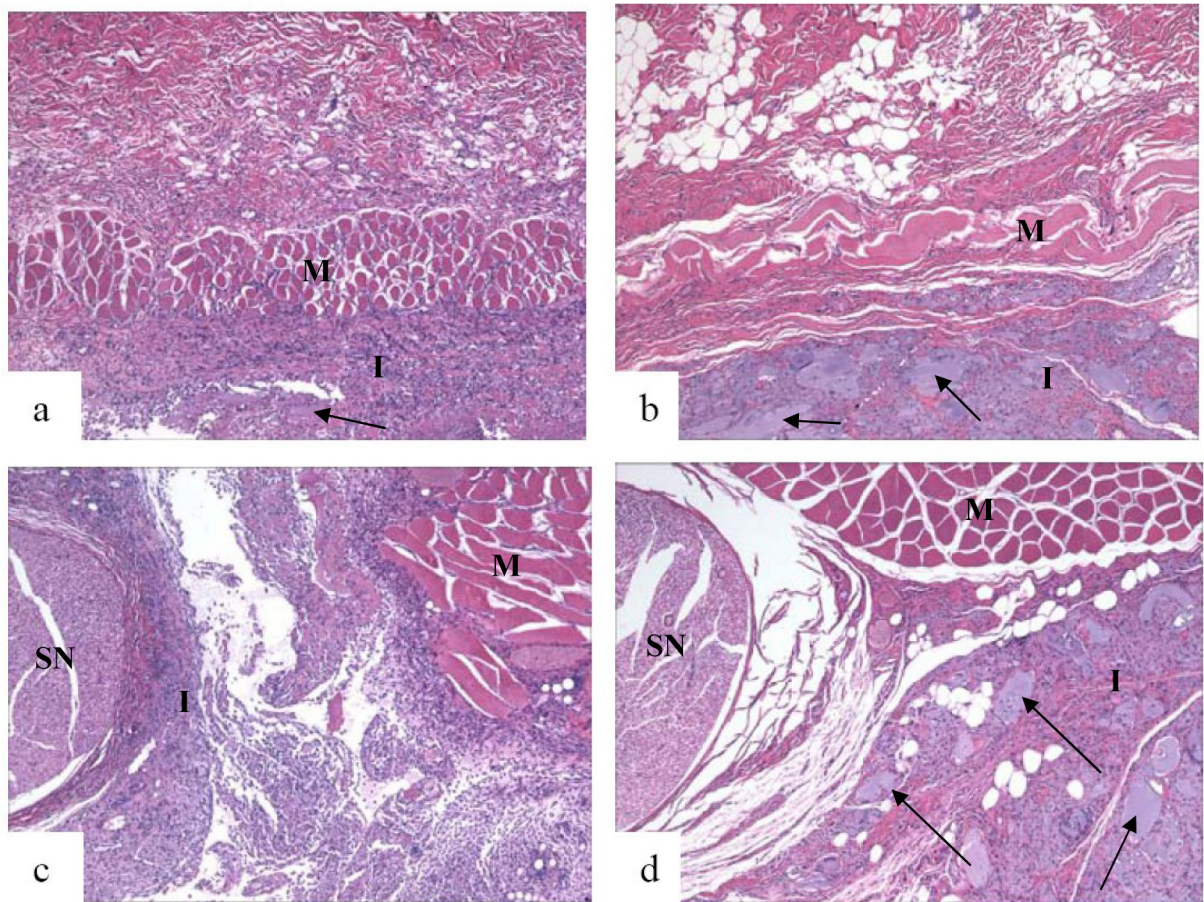


Figure 8.

Light microscopy of subcutaneous nodules of SBA-15 at (a) 4 days and (b) 3 months and sciatic nerve injection site of SBA-15 at (c) 4 days and (d) 3 months. Arrows indicate MPS material, SN – sciatic nerve, M – muscle, I – inflammation. All images are 40x the original magnification.

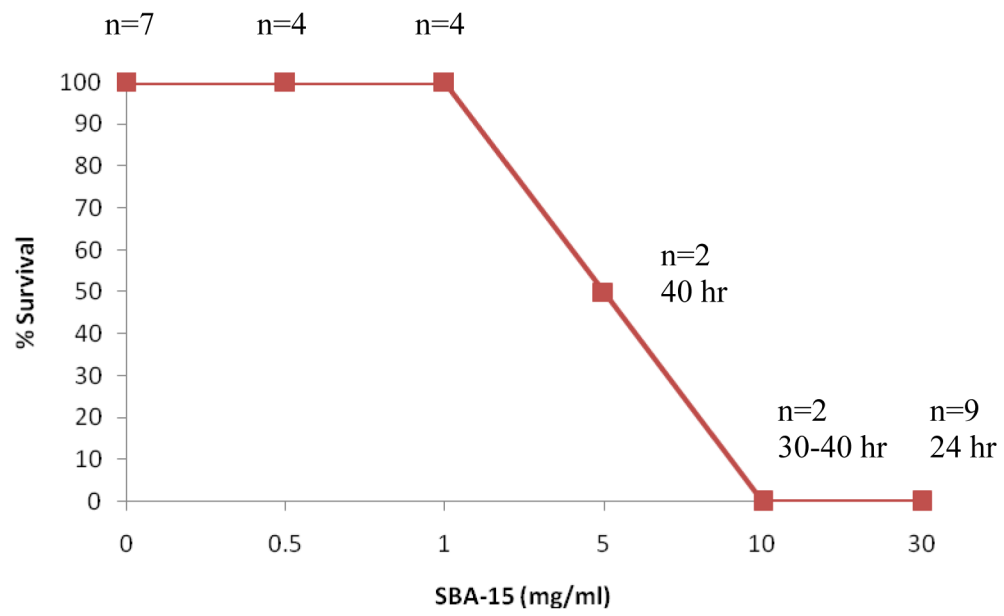


Figure 9. Percentage survival of mice injected intraperitoneally with 1 ml of SBA-15 suspension.

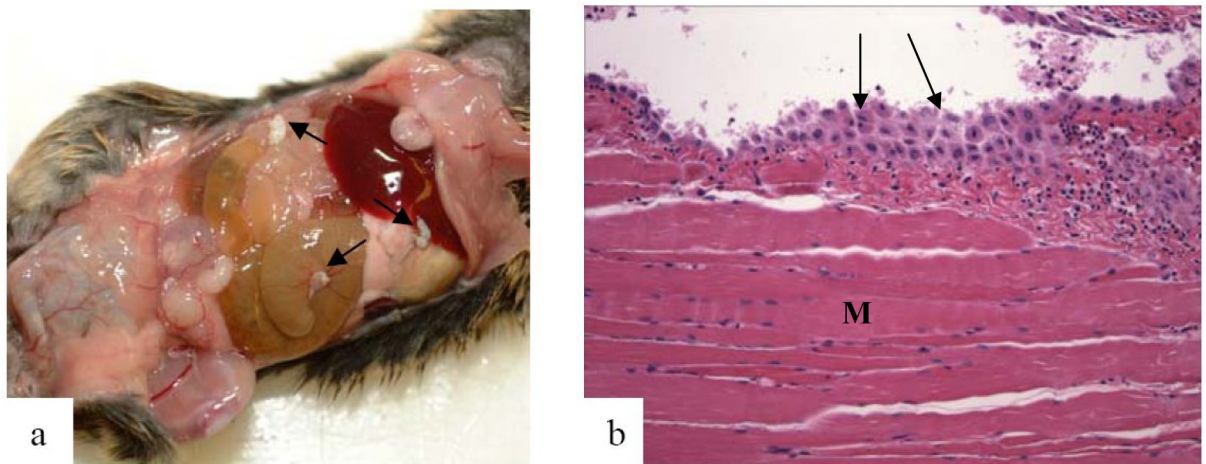


Figure 10.

(a) Mouse peritoneum 24 hours after IP injection with MCM-41_{ref} (30 mg). Arrows indicate small pockets of residue. (b) Light microscopic tissue analysis of mouse peritoneum after SBA-15 (30 mg) IP injections. Arrows indicate mesothelial cells, M – abdominal muscle. Image (b) is 100x the original magnification.

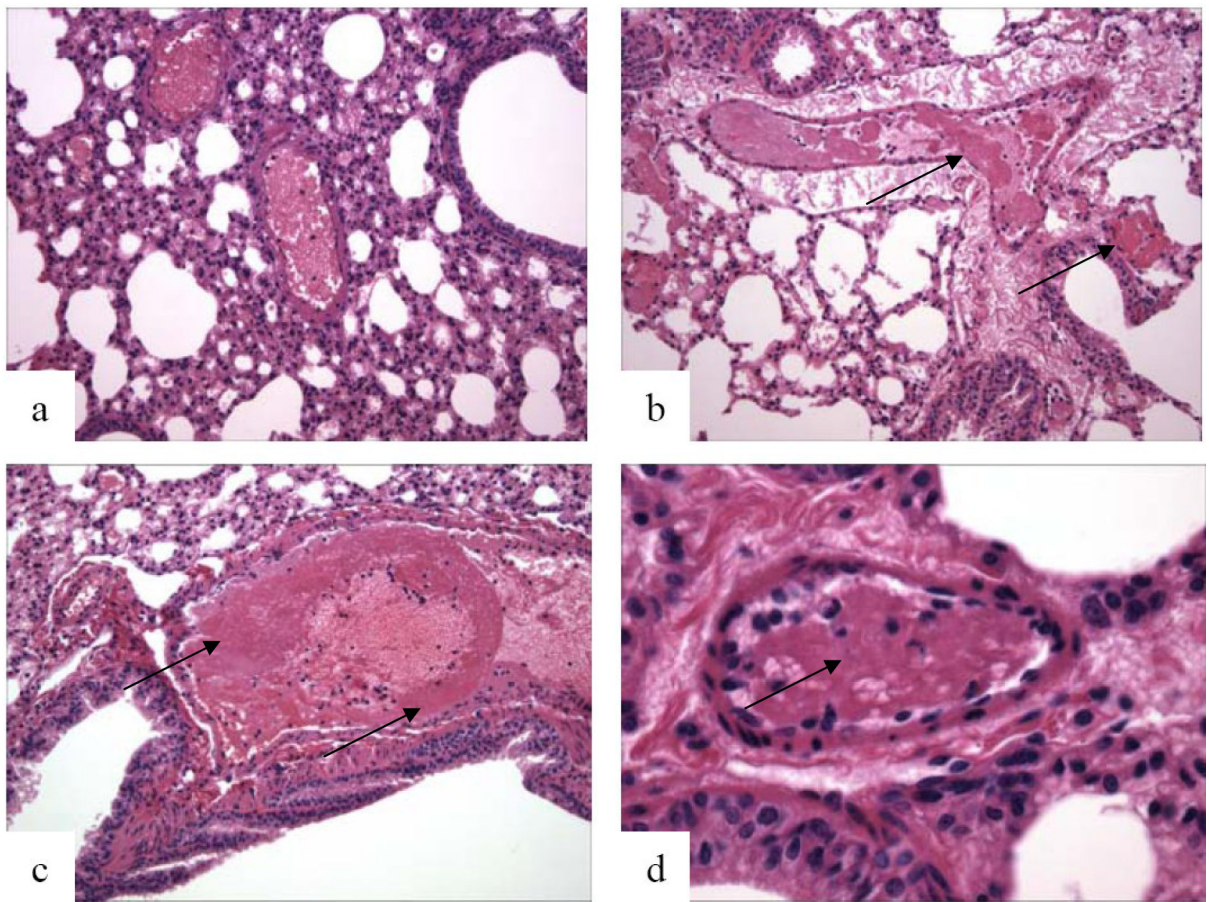


Figure 11.

Light microscopy of lung tissue from mice after injection of (a) 1% CMC control intraperitoneally, (b) MCM-41_{ref} (6 mg) intravenously, (c) and (d) MCM-41_{ref} (30 mg) intraperitoneally, low and high magnification respectively. Arrows indicate blood clots. Images (a–c) are 100x and (b) is 400x the original magnification.

Table 1
Physicochemical properties and elemental analyses of mesoporous silicate

Mesoporous silicate	Surface Area (m ² /g)	Pore Size* (nm)	Pore Size** (nm)	Unit Cell Parameter (nm)	Elemental analysis		
					%C	%H	%N
MCM-41 _{ref}	650	3.1	3.2	4.6	0.73	1.72	<0.05
MCM-41 _{cal}	947	2.7	2.8	4.2	0.97	0.68	<0.05
SBA-15	586	7.2	9.9	12.2	4.46	1.91	<0.05
MCF	475	16	40	-	2.41	1.24	<0.05

* Calculated from the desorption branch

** Calculated from the adsorption branch

Table 2

Particle sizes of mesoporous silicates as measured using SEM, Zetasizer and Coulter Counter equipment.

Material	Method of Measurement		
	SEM (nm)	Zetasizer (nm)	Coulter counter (nm)
MCM-41 _{ref}	100–150	470±252	-
MCM-41 _{cal}	100–150	270±38	-
SBA-15	600–800	740±160	-
MCF	4000–5000	4700±1150	5270±4000

Table 3

Mortality of MPS in rats

Material ^a	Mortality ^b	Time to death ^c	Numbers of animals euthanized for necropsy, by time point					
			4 days	2 wks	1 mo	2 mos	3 mos	
MCM-41 _{gal}	1 of 8	2 days	2	2	-	2	2	
MCM-41 _{red}	1 of 6	3 days	2	2	1	1	-	
SBA-15	0 of 14	-	4	4	1	3	2	
MCF	0 of 14	-	4	4	1	3	2	

^a 60 mg of MPS were injected subcutaneously and at the sciatic nerve in the same animal.

^b From presumed MPS toxicity; not by euthanasia.

^c In animals that died from presumed MPS toxicity.

Table 4

Mortality rate of mice after injection of mesoporous silicates.

Route of Injection	Material	Dose (mg)	Mortality	Time to death
Intraperitoneal*	MCM-41 _{cal}	30	8 of 8	24 hrs
	MCM-41 _{ref}	30	4 of 4	24 hrs
	SBA-15	30	9 of 9	24 hrs
	MCF	30	8 of 8	24 hrs
	1%CMC		0 of 7	-
	Supernatant from MCM-41 _{ref}		0 of 2	-
Subcutaneous*	Supernatant from SBA-15		0 of 3	-
	MCM-41 _{ref}	30	0 of 4	-
	MCM-41 _{cal}	30	0 of 2	-
	SBA-15	30	0 of 2	-
Intravenous**	MCM-41 _{ref}	6	2 or 2	<15 mins

* Injected in 1% CMC.

** Injected in phosphate buffered saline.